Scientific Journal for Damietta Faculty of Science **14**(3) 2024, 90-101
doi: 10.21608/sjdfs.2025.332686.1193
ISSN Print 2314-8594
ISSN Online 2314-8616

https://sjdfs.journals.ekb.eg/

Antibacterial Activity of Green Synthesized Zinc Oxide Nanoparticles using *Washingtonia Robusta* H. Wendl Fruit Extract

Rolla M. Fayed[1], Zakaria A. M. Baka[1] and Mohamed M. El-Zahed[*1]

[1]Department of Botany and Microbiology, Faculty of Science, Damietta University, Egypt.

Received: 31 October 2024 /Accepted: 05 December 2024

[*]Corresponding author's E-mail: Mohamed.marzouq91@du.edu.eg

Abstract

Bacterial infections remain a critical global health concern, often leading to prolonged self-medication, extended healing times, treatment failures, increased hospitalization, and higher healthcare costs, alongside increased mortality rates. Recent research efforts have focused on enhancing human health and environmental sustainability through innovative synthesis techniques. This study presents a straightforward and cost-effective method for the green synthesis of zinc oxide nanoparticles (ZnO NPs) using fruit extract from *Washingtonia robusta* H. Wendl and investigated their antibacterial activity. The *W. robusta* fruit extract underwent fractionation using polar and non-polar solvents, resulting in the isolation of four distinct fractions that were tested against various Gram-positive and Gram-negative bacteria as antibacterial agents. The methanolic fraction demonstrated the highest antibacterial potential and was analyzed for bioactive compounds using gas chromatography-mass spectrometry (GC-MS). This analysis identified ten biochemical constituents, including hexasiloxane (43.28%), E-9-tetradecenoic acid (12.99%), oleic acid (10.12%), and heptasiloxane (9.83%). This methanolic fraction was utilized in the synthesis of ZnO NPs. The resulting nanoparticles were characterized using various techniques, including UV-Vis spectroscopy, FTIR spectroscopy, zeta analysis, and transmission electron microscopy (TEM). The antibacterial efficacy of the ZnO NPs was evaluated against *Escherichia coli* ATCC25922, and *Bacillus cereus* ATCC6633. The antibacterial activity was assessed using the agar well diffusion method, minimum inhibitory concentration (MIC), and minimum bactericidal concentration (MBC). Results indicated that the ZnO NPs exhibited a good antibacterial activity with average inhibition zones 18 ± 0.03 mm against *E. coli*, and 24 ± 0.14 mm against *B. cereus*. The MIC values for ZnO NPs were 35 µg/ml against *E. coli* and 25 µg/ml against *B. cereus*. The MBC values matched with MIC results that indicated the potent bactericidal action of the prepared ZnO NPs.

Keywords: Washingtonia robusta, zinc oxide nanoparticles, GC–MS, antibacterial activity.

Introduction

Antimicrobial resistance (AMR) occurs when microorganisms such as bacteria, fungi, and parasites acquire resistance to antimicrobial treatments in people and animals. AMR has

grown into a severe concern, influencing illness treatment and increasing mortality rates **(Prestinaci *et al*., 2015)**. It has become a persistent global public health issue, with a projected 10 million fatalities per year worldwide by 2050 **(Tripathi *et al*., 2019)**. This issue is ascribed to the excessive and inappropriate use of antimicrobial agents, particularly antibiotics, which contributes to the global burden of antimicrobial resistance. As a result, antibiotic use and consumption are constantly and thoroughly monitored around the world **(Tang *et al*., 2023)**. The development of innovative antimicrobial medicines to counteract persistent disease progression has been the subject of numerous investigations in recent years. Furthermore, the European Food Safety Authority (EFSA) has found that some bacteria such as *Escherichia coli*, *Pseudomonas aeruginosa*, *Bacillus cereus*, and *Klebsiella pneumoniae*, are becoming less vulnerable to the existing antibiotics, including fluoroquinolones **(Silva *et al*., 2024)**. The term "high-risk clone" describes bacterial strains that accelerate the development of antibiotic resistance. Since E. coli has become a storehouse of genes resistant to different antibiotics, the World Organization for Animal Health (WOAH) acknowledges that it is an essential indication for tracking the spread of antibiotic resistance **(De Lagarde *et al*., 2021)**. Since these strains are extremely effective at carrying mobile genetic elements, such as genes that provide resistance to antibiotics, which speeds up the spread of these genes, they are a serious cause for concern. Furthermore, they present serious difficulties while treating patients **(Tiwari *et al*., 2023)**.

Herbal therapy has been suggested as a secure and efficient way to deal with this issue. Medicinal plants frequently contain polypeptides, flavonoids, coumarins, terpenoids, alkaloids, tannins, polyphenols, and essential oils **(Leisegang, 2021)**. The fabrication of antibiotics and the management of many diseases are facilitated by these secondary metabolites **(Abutaha *et al*., 2023)**. Palms yield a variety of beneficial goods and are rich in terpenoids, phenolic compounds, and oils. Pro-vitamin A, tocols, vitamin E, and triterpene pentacyclics are among the terpenoids and other volatile substances found in the mesocarp and endocarp oils of certain palms that have been linked to health advantages. The phenolic chemicals that include phenolic acids, resveratrol, other stilbenes, anthocyanins, flavones, flavonols, dihydroflavonoids, flavan-3-ol, procyanidins, and lignansthat have been identified in various tissues of this palm, particularly in the pulp, seeds, and leaves **(Da Silveira, 2018)**. According to **Selim *et al*. (2020)**, *Washingtonia robusta* produces several phytochemical substances with antibacterial properties, including n-hexadecanoic acid, 1,2,3-propanetriol, and 1-acetate. However, during the biofilm-forming process, several bacteria, such as *S. aureus* and *E. coli*, show resistance to certain phytochemical substances **(Monte *et al*., 2014; Silva *et al*., 2024)**. Furthermore, combining phytochemical substances with other antibiotics, including tetracycline, erythromycin, salicylic acid, and saponins, did not result in a synergistic impact against S. aureus-resistant strains **(Monte *et al*., 2014)**.

Presently, technological developments such nanotechnology might enhance the health benefits of these phytochemicals and encourage their use **(Álvarez-Martínez *et al*., 2020; Díaz-Puertas *et al*., 2023)**. Nanomaterials (1 to 100 nm) are a remarkable category of materials with a range of unique physicochemical and biological properties when compared to bulk materials of larger scale **(Fayed *et al*., 2023)**. Nanomaterials are produced using different chemical and physical methods, including the sol-gel method, thermal breakdown, chemical vapor deposition, laser ablation, and microwave synthesis (Khan, 2020). Nevertheless, it was discovered that the artificial nanomaterials created using earlier techniques were harmful to human cells and might have detrimental consequences on medicinal applications. As an alternative, biological methods that employ plants and other microbes during biosynthesis have produced biocompatible, stable, and nontoxic nanomaterials **(Raina *et al*., 2020)**. Various medical applications of metal-based nanoparticles (NPs) have been investigated. According to the World Health Organization (WHO), metal-based NPs have the potential for combating priority-listed diseases moreover their small size and improved bacterial selectivity. They have nonspecific bacterial toxicity mechanisms because they do not attach to a specific receptor in the bacterial cells. This prevents the growth of bacterial resistance and increases the range of antibacterial activity **(Sánchez-López *et al*., 2020)**. due to their solid state and ability to treat wounds with salt

solutions, a variety of NPs with antibacterial activity, such as silver, gold, copper, and manganese NPs, have been employed as antimicrobial agents for wound healing **(Chen and Schluesener, 2008)**. Biomedicine, the food industry, textiles, and cosmetics are among the majority of the industries that use nanomaterials. Their prospective uses as antibacterial agents, medical device coatings, and chemotherapeutic drug carriers have contributed to their increasing popularity in the biomedical sector **(Chen and Schluesener, 2008; Sengul and Asmatulu, 2020)**. However, despite their strong antibacterial action, these metals or their metal oxide nanoparticles have serious negative consequences. Some research indicates that the primary target tissues for extended exposure to silver nanoparticles (AgNPs) are the liver and lungs **(Hadrup and Lam, 2014)**. It can release silver ions that can result in cytotoxicity, genotoxicity, and even cell death because of its capacity to interact with biological systems and pass-through cell membranes **(De Lima *et al*., 2012; Zhang *et al*., 2014)**. Due to gold NPs (AuNPs), Because they are less harmful to mammalian cells than AgNPs and efficient against both Gram-positive and Gram-negative bacteria, they are the most frequently used antimicrobial agents. However, some researchers are investigating into the possible antibacterial activity of AuNPs. In addition to their antibacterial properties, AuNPs also have antioxidant and anticancer effects **(Sánchez-López *et al*., 2020)**. These NPs cause microbial DNA damage and cell death, and promote the production of endogenous reactive oxygen species (ROS) **(Sánchez-López *et al*., 2020; Tiwari *et al*., 2011)**. Conversely, zinc (Zn) and zinc oxide (ZnO) have emerged as powerful antibacterial agents in various pharmaceutical and industrial applications, including paint, paper, cosmetics, plastics, building materials, and ceramics. Their desirable characteristics, such as high stability, antimicrobial efficacy, and anticorrosive properties, make them effective alternatives in the biomedical field. Zinc also plays a crucial role in various biological functions, such as supporting immune health, promoting wound healing, and acting as an antioxidant. Additionally, both zinc and zinc oxide are cost-effective, safe, exhibit low toxicity, and possess strong UV absorption capabilities **(Tulinski and Jurczyk, 2017)**. Their antibacterial activity is enhanced when combined with other compounds. Zinc ions interact with biological macromolecules, leading to damage to bacterial cell walls, inhibition of bacterial cell reproduction, disruption of protein synthesis, reduction of membrane permeability, and interference with bacterial metabolic functions **(El-Fallal *et al*., 2023)**. The current study aimed to green-synthesize zinc oxide (ZnO) using *W. robusta* fruit extract at room temperature (25°C) and investigate there antibacterial efficacy against Gram-positive and Gram-negative bacteria.

Material and Methods

Sample collection

Fresh *W. robusta* fruits were collected during the autumn season (October 5th, 2023) from palms in New Damietta City, Damietta Governorate, Egypt, and taken to the Microbiology Laboratory at the Faculty of Science, Damietta University, for extraction. They were round to oval, roughly 1.27 cm long, and had a fleshy crust that was black to dark brown (Figure 1). The fruits were carefully washed to remove any dirt, and any damaged seeds were discarded before drying. The healthy, mature fruits were then ground into a fine powder and stored in glass containers at 4°C for subsequent physicochemical analysis **(Gomaa, 2019)**.

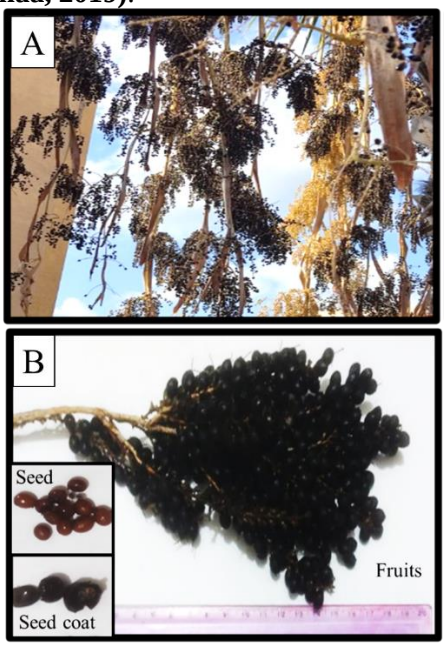

Figure 1. *Washingtonia robusta* H. Wendl (left) and its fruits (right) that used in the current study.

Plant sample preparation and extraction

The fruits of *W. robusta* were crushed using a hammer, then blended and sieved through a 30-mesh stainless steel screen. To ensure a consistent powder, the remaining residue was blended again until all of it passed through the screen. Five grams of this powder were homogenized with 40 ml of methanol for 1 minute and extracted on a shaker for 3 hours at room temperature (25°C) **(Gomaa, 2019)**. The resulting extracts were hydrolyzed with 3 M HCl and fractionated using polar and non-polar solvents at the Center for Excellence in Research of Advanced Agricultural Sciences (CERAAS), Damietta University, Egypt.

Antibacterial activity of fractionated-fruit extracts using agar well diffusion method

The agar well diffusion method was used to assess the fruit extracts' antibacterial activity in accordance with the Clinical and Laboratory Standards Institute (CLSI) protocol **(CLSI, 2017)**. *E. coli* ATCC25922 and *B. cereus* ATCC6633 were used as bacterial models. A 0.5 McFarland standard (1-2 x 10^8 CFU/ml) from each bacterial strain was prepared. These microbes were inoculated into cooled melted nutrient agar medium flasks, which were then poured into sterile Petri dishes and allowed to solidify. Using a cork borer, wells were made in each plate, and 100 µl of each fractionated extracts were added to the wells under aseptic conditions. After incubation at 37°C for 24 hours, the inhibition zones around the wells were measured in millimeters.

Gas chromatography-mass spectrometry (GC-MS) analysis

The phytochemicals extracted from the fruits of *W. robusta* H. Wendl were identified at the CERAAS, Damietta University, Egypt. GC-MS analysis of extract was carried out in accordance with **Elbestawy *et al*. (2023)**. A GC-MS system (TSQ 9000 triple quadrupole mass spectrometer was coupled to a Thermo Scientific™ TRACE™ 1310 Gas Chromatograph) fitted with a 30 m × 0.25 mm Rtx-5 MS column (0.25 µm film thickness) was used to examine the extract's chemical makeup. With an injection volume of 1.0 µL and a split ratio of 10:1, Helium functioned as the carrier gas at a steady flow rate of 1.2 mL/min. At 70 eV, the ionization mass analysis was carried out. The ion source temperature was kept at 280°C while the injector temperature was adjusted to 250°C. The oven temperature programming started with an initial isothermal phase at 110°C for two minutes, followed by increases of 10°C/min to 200°C, then 5°C/min to 280°C, and finally held isothermally at 280°C for nine minutes. Data was collected using the GC-MS post-run software.

Green synthesis of zinc oxide nanoparticles (ZnO NPs)

Zinc nitrate hexahydrate solution (10 mM) was prepared, mixed with the selected *W. robusta* H. Wendl fruit extract at a ratio of 1:1 (v/v%) and shaken well (200 rpm) at room temperature (25°C ± 2) for 15 min until the colour change of the solution from pale yellow and white precipitate formation indicated the formation of ZnO NPs **(Song *et al*., 2022)**.

Characterization of ZnO NPs

The green-synthesized ZnO NPs were analyzed using several techniques, including UV/Vis Spectrophotometer (Beckman DU-40) and Fourier transform infrared spectroscopy (FTIR, FT/IR-4100 type A). Additional analyses included zeta potential measurements (Malvern Zetasizer Nano-ZS90, Malvern, UK), and transmission electron microscopy (TEM, JEOL JEM-2100, Japan).

Antibacterial activity of ZnO NPs using agar well diffusion method

Different concentrations (250, 500, and 1000 µg/ml) of ZnO NPs were evaluated for their antibacterial activity against the selected bacterial strains using the agar well diffusion method, in accordance with the Clinical and Laboratory Standards Institute **(CLSI, 2017)**. Penicillin G was used as a control antibiotic. The methanolic fraction of fruit extract was also included in the testing.

Minimal inhibitory concentration (MIC)

The broth microdilution method was used to evaluate the MICs of ZnO NPs in accordance with CLSI recommendations **(CLSI, 2000)**. *B. cereus* and *E. coli* were cultivated on Mueller-Hinton broth (MHB) at a 0.5 McFarland

standard. Serial solutions (0-100 µg/ml) from ZnO NPs, and penicillin G were prepared and tested. The microorganisms under the test were cultured for 48 hours at 37°C. After incubation time, the turbidity of bacterial growth was evaluated at 630 nm using a spectrophotometer in comparison to the growth control.

Minimum bactericidal concentration (MBC)

Each MIC bacterial flask was inoculated into Mueller-Hinton agar plates using the pour plate method and incubated at 37°C for 24 hours. Every bacterial colony's total count was measured in colony-forming units per milliliter (CFU/ml) **(El-Zahed *et al*., 2024)**.

Statistical analysis

Statistical analysis of the data was conducted using SPSS version 18 software. Each experimental value is presented as the mean ± standard deviation (SD), and one-way analysis of variance (ANOVA) was employed for the analysis. A significant level of $p<0.05$ was established. All experiments were performed in triplicate.

Results

Antibacterial activity of fractionated extracts of W. robusta H. Wendl fruit

Methanolic, ethyl acetate, n-hexane, and chloroform extracts were separated into four fractions. The antibacterial activity of the fractionated-extracted fractions was assessed against various Gram-positive and Gram-negative bacteria, as shown in Table 1. The methanolic extract demonstrated significantly greater antibacterial activity against Gram-negative bacteria than against Gram-positive bacteria. It was particularly effective against *E. coli* ATCC25923, exhibiting an inhibition zone of 15 mm compared to *B. cereus*, exhibiting an inhibition zone of 12 mm. In contrast, the n-hexane extract displayed the lowest antibacterial activity against both bacterial strains. The ethyl acetate extract also showed weaker antibacterial effects compared to the methanolic extract. On the other hand, ethyl acetate did not affect *E. coli*.

Table 1. The agar well diffusion method of fractionated extract of *W. robusta* H. Wendl fruits against the tested bacteria.

Fractions	**Inhibition zone in mm (mean ± SD)**	
	Gram-negative bacterium	Gram-positive bacterium
	E. coli	*B. cereus*
n-Hexane	6 ± 0.16	9 ± 0.14
Chloroform	12 ± 0.14	10 ± 0.06
Ethyl acetate	-ve	8 ± 0.16
Methanol	15 ± 0.06	12 ± 0.03

Chemical composition of methanolic fraction of fruit extract using GC–MS analysis

Ten different compounds were found during the GC-MS screening of the methanolic extract of *W. robusta* H. Wendl fruits (Figure 2 and Table 2). hexasiloxane (43.28%), E-9-tetradecenoic acid (12.99%), oleic acid (10.12%), and heptasiloxane (9.83%), trimethylsiloxyphenylsiloxane (8.36%), decanoic acid (4.02%), and 2-isoxazolin-5-one, 3-phenyl (3.89%) were the main constituents.

Table 2. Chemical profile of methanolic *W. robusta* H. Wendl fruit extract by GC–MS.

Peak	Retention time	Peak Area %	Compound name	Molecular formula	Molecular weight
1	7.28	2.25	1,2,3-Propanetriol,1-acetate	$C_5H_{10}O_4$	134
2	9.67	3.89	2-Isoxazolin-5-one, 3-phenyl	$C_9H_7NO_2$	161
3	17.92	4.02	Decanoic acid	$C_{19}H_{36}O_2$	296
4	21.05	2.21	Phenytoin	$C_{15}H_{12}N_2O_2$	252
5	23.88	3.05	psi.,.psi.-Carotene, 3,4-didehydro-1,2-dihydro-1-methoxy	$C_{41}H_{58}O$	566
6	26.28	12.99	E-9-Tetradecenoic acid	$C_{14}H_{26}O_2$	226
7	26.61	10.12	Oleic Acid	$C_{18}H_{34}O_2$	282
8	30.07	8.36	Bis[di(trimethylsiloxy)phenylsiloxy]trimethylsiloxyphenylsiloxane	$C_{33}H_{60}O_7Si_8$	792
9	38.03	9.83	Heptasiloxane,1,1,3,3,5,5,7,7,9,9,11,11,13,13-tetradecamethyl	$C_{14}H_{44}O_6Si_7$	504
10	43.75	43.28	Hexasiloxane, 1,1,3,3,5,5,7,7,9,9,11,11-dodecamethyl	$C_{12}H_{38}O_5Si_6$	430

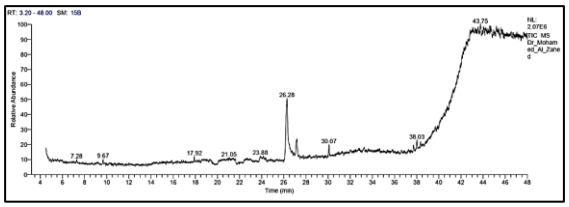

Figure 2. GC–MS analysis of the methanolic extract of *W. robusta* H. Wendl fruits.

Synthesis and characterization of the ZnO NPs

The formation of the NPs was first indicated by a color change in the reaction mixture to bright yellow, as illustrated in Figure 3. Within 10 minutes, a white precipitate of ZnO NPs emerged, confirming their successful green synthesis. Also, an absorption peak at 347 nm was observed at the UV-Vis spectrum (Figure 3).

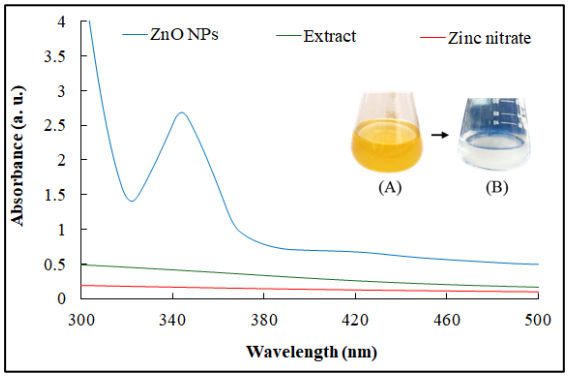

Figure 3. Color change and UV–Vis spectroscopy analysis of the ZnO NPs. (A) Color of the reaction mixture at the beginning of the experiment. (B) Color changes to a white color due to the formation of ZnO NPs.

FTIR spectroscopy was employed to verify the successful formation of ZnO NPs and to identify the presence of capping agents during the synthesis process. The spectrum (Figure 4) showed a broad peak at 3356 cm^{-1}, which corresponds to the O–H stretching vibration of methanol, the solvent used. Stretching peaks at 2994 and 2938 cm^{-1} were linked to secondary amines. Additional peak at 1636 cm^{-1} indicated the presence of vinyl and cis-trisubstituted groups, while amine stretching vibrations were observed at 1457 and 1369 cm^{-1}. C–O stretching vibrations were noted at 822 cm^{-1}. The Zn–O stretching vibration was detected at approximately 648 cm^{-1}.

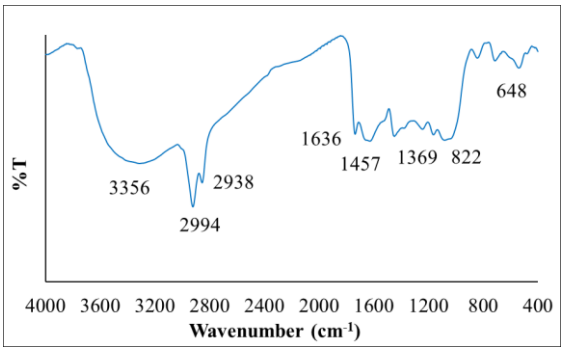

Figure 4. FTIR of the green synthesized ZnO NPs.

The Zeta potential analysis revealed a negative charge of -27.4 mV for the ZnO NPs (Figure 5).

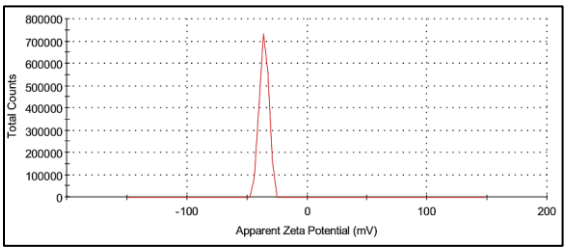

Figure 5. Zeta potential analysis of ZnO NPs.

TEM micrograph of the obtained ZnO NPs are presented in Figure 6. The NPs displayed a spherical morphology, with an average diameter of 26.21 nm.

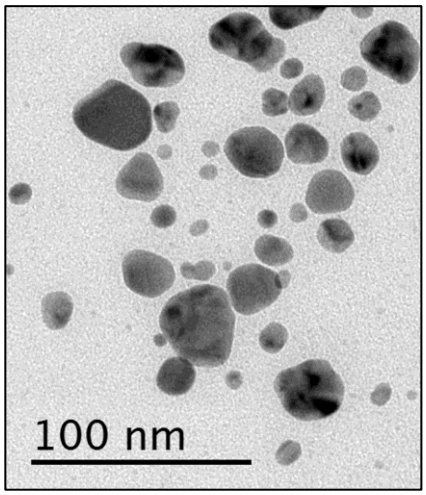

Figure 6. TEM of ZnO NPs with scale bar = 100 nm.

Antibacterial activity of the ZnO NPs

The antibacterial action of green-synthesized ZnO NPs was evaluated and compared to that of methanolic fraction of fruit extract and penicillin G as a reference drug. All bacterial strains tested exhibited susceptibility to both ZnO NPs and penicillin G (Table 3). The methanolic fraction showed limited antibacterial activity, while ZnO NPs

demonstrated significantly stronger biocidal effects against Gram positive bacteria compared to Gram negative bacteria. The Gram-positive bacterium *B. cereus* was particularly affected by ZnO NPs, displaying an inhibition zone of 24 ± 0.14 mm, whereas Gram-negative bacterium *E. coli* showed a smaller inhibition zone 18 ± 0.03 mm.

Table 3. Agar well diffusion of ZnO NP against the tested bacteria.

Antibacterial agent	**Concentration, µg/ml**	**Inhibition zone in mm (mean ± SD)**	
		Gram-negative bacterium	Gram-positive bacterium
		E. coli	*B. cereus*
Methanolic fraction	250	6 ± 0.12	-ve
	500	10 ± 0.14	7 ± 0.18
	1000	14 ± 0.12	10 ± 0.06
ZnO NPs	250	20 ± 0.16	11 ± 0.14
	500	22 ± 0.14	15 ± 0.06
	1000	24 ± 0.14	18 ± 0.03
Penicillin G	250	15 ± 0	12 ± 0
	500	18 ± 0	14 ± 0
	1000	21 ± 0	16 ± 0

The MICs of ZnO NPs and penicillin G against *E. coli* and *B. cereus* were assessed (Figure 7). ZnO NPs completely inhibited *B. cereus* at 25 µg/ml and *E. coli* at 35 µg/ml. In comparison, penicillin G inhibited *B. cereus* at 30 µg/ml and *E. coli* at 40 µg/ml. The MBC values for penicillin G were 35 µg/ml for *B. cereus* and 45 µg/ml for *E. coli*, while the MBCs for ZnO NPs were consistent with their MICs.

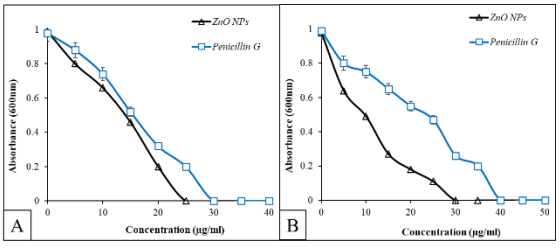

Figure 7. The minimum inhibition concentrations of ZnO compared to penicillin G against *E. coli*; (A) and *B. cereus*; (B).

Discussion

New antibacterial medications with potent and long-lasting action are required due to the rapidly growing bacterial resistance. *W. robusta* H. Wendl fruits were used to prepare an antibacterial plant extract which contains several bioactive compounds as recommended by previous studies **(Abutaha *et al.*, 2023; Gomaa, 2019; Selim *et al.*, 2020)**. Most of the compounds identified in GC-MS analysis were also reported in **Dewir *et al.* (2021)** study, including oleic acid (40.6%), 1,2,3-propanetriol,1-acetate (3.47%), hydrazine carboxamide (1.67%), decanoic acid (6.47%), n-hexadecanoic acid (6.47%), and octasiloxane (1.18%). Several of these compounds are 1,2,3-propanetriol,1-acetate, decanoic acid, oleic acid, phenytoin, n-hexadecanoic acid, and octasiloxane are known for their inhibitory effects on both Gram-positive and Gram-negative bacteria **(Novak *et al.*, 1961; Saeed *et al.*, 2023; Venkatesh *et al.*, 2014)**. **Foo *et al.* (2015)** also reported that 1,2,3-propanetriol,1-acetate exhibited antibacterial activity against *B. cereus*, while n-hexadecanoic acid showed effectiveness against *Staphylococcus aureus* ATCC 25923, *E. coli* ATCC 4102, and *Salmonella* sp. ATCC 50041 **(Pu *et al.*, 2010)**. The results obtained for the antibacterial activity of methanolic fraction of fruit extract are consistent with earlier studies, such as those conducted by **Abutaha *et al.* (2019)**, who found that the methanolic extract of *W. filifera* (Lindl.) H. Wendl. fruit displayed stronger antibacterial activity against *E. coli*, *K. pneumoniae*, *Acinetobacter baumannii*, and *S. aureus* compared to other extracts like chloroform, ethyl acetate, and hexane. They reported that the methanolic extract was especially effective against S. aureus, achieving an inhibition zone of 30 mm, which exceeded the 20 mm inhibition zone noted for *E. coli*. Furthermore, **Adegoke *et al.* (2010)** observed that methanolic extracts demonstrated greater antibacterial activity against *S. aureus* ATCC25923 (inhibition zone: 15 mm) than against *Salmonella typhi* (inhibition zone: 8 mm) when compared to chloroform extracts. These findings indicate that methanolic extracts are generally more effective against specific bacterial strains than extracts from other solvents.

The observed color change during the synthesis process clearly indicates the successful formation of ZnO NPs. The white color of the obtained ZnO NPs appeared throughout 10 minutes after mixing methanolic fraction of *W. robusta* H. Wendl fruits extract with zinc nitrate solution. The appearance of a white precipitate confirms their presence and is attributed to the Surface Plasmon Resonance (SPR) effect. The

specific absorption peaks at 347 nm and 361 nm verify the optical characteristics of ZnO NPs, which is consistent with prior research highlighting the importance of SPR in nanoparticle analysis consistent with the results of **Saleem *et al*. (2022)**. While **Lee *et al*., (2008)** documented the synthesis of ZnO NPs displayed absorption peak at 361 nm. These results affirm the effectiveness of the synthesis method used to produce ZnO NPs.

The current study recorded a good activity for the green synthesized ZnO NPs. Also ZnO NPs exhibited significant antibacterial activity against *S. aureus*, achieving a 30 mm inhibition zone as reported by **Ahmad *et al*. (2020)**. In another study, **Song *et al*. (2022)** reported that the MICs of ZnO/Se were 312.5 µg/ml for *S. aureus* and 625 µg/ml for *E. coli*. **Xia *et al*. (2022)** observed that at a concentration of 1000 µg/ml, the bacteriostatic rates of ZnO NPs against *E. coli* were 92.94% and 87.34%, respectively, while the rates against *S. aureus* were 58.94% and 55.64%. Microscopic analysis revealed a separation between the bacterial cell wall and cell membrane in bacteria treated with ZnO NPs.

ZnO NPs are well-known antimicrobial agents that primarily target bacteria through oxidative stress. The production of ROS leads to the rupture of the bacterial cell wall, resulting in the release of proteins and nucleic acids. ROS also oxidizes key proteins like glutathione, disrupting major respiratory enzymes, which leads to bacterial cell death **(Applerot *et al*., 2009; El-Dein *et al*., 2021)**. Effective nanometallic materials, ZnO NPs cause bacterial membranes to become unstable, increasing cell permeability to NPs. They have shown a lot of promise as all-purpose antibacterials. However, further engineering is required to minimize their toxicity to healthy cells and optimize their biological function **(Glover *et al*., 2021)**.

Conclusions

This study presents a straightforward and eco-friendly method for synthesizing ZnO NPs using methanolic extract of *Washingtonia robusta* H. Wendl fruit as both a stabilizing and reducing agent. The synthesis of ZnO NPs was confirmed using UV-Vis spectroscopy, FTIR, zeta analysis, and TEM. The zeta potential and FTIR analysis of the ZnO NPs demonstrated their long-term stability. The green-synthesized ZnO NPs showed potent antibacterial activity against both Gram-negative and Gram-positive bacteria, with MIC values ranging from 25 to 35 µg/ml. In comparison, penicillin G exhibited higher MIC values between 30 and 40 µg/ml. Based on the results from the agar well diffusion assay, MIC, and MBC, it was observed that Gram-positive bacteria were more sensitive to ZnO NPs than Gram-negative bacteria that might use in different medical and pharmaceutical applications.

References

Abutaha, N., AL-mekhlafi, F.A., Wadaan, MA., 2023. Phytochemical analysis and antibacterial activity of *Washingtonia filifera* (Lindl.) H. Wendl. fruit extract from Saudi Arabia. J. King Saud Univ. Sci. 35(8), 102899. https://doi.org/10.1016/j.jksus.2023.102899

Adegoke, S.A., Opata, O.M., Olajide, J.E., 2010. Antimicrobial activity of the aqueous, methanol and chloroform leaf extracts of *Cissus multistriata*. Afr. J. Biotechnol. 9(8), 1168-1172. https://doi.org/10.5897/AJB2010.000-3012

Ahmad, A., Ullah, S., Ahmad, W., Yuan, Q., Taj, R., Khan, A.U., Rahman, A.U., Khan, U.A., 2020. Zinc oxide-selenium heterojunction composite: Synthesis, characterization and photoinduced antibacterial activity under visible light irradiation. J. Photochem. Photobiol. B 203, 111743. https://doi.org/10.1016/j.jphotobiol.2019.111743

Alam, H., Khatoon, N., Khan, M.A., Husain, S.A., Saravanan, M., Sardar, M., 2020. Synthesis of selenium nanoparticles using probiotic bacteria *Lactobacillus acidophilus* and their enhanced antimicrobial activity against resistant bacteria. J. Clust. Sci. 31, 1003-1011. https://doi.org/10.1007/s10876-019-01705-6

Álvarez-Martínez, F.J., Barrajón-Catalán, E., Encinar, J.A., Rodríguez-Díaz, J.C., Micol, V., 2020. Antimicrobial capacity of plant polyphenols against Gram-positive bacteria: A comprehensive review. Curr. Med. Chem. 27(15), 2576-2606. https://doi.org/10.2174/0929867325666181008115650

Amooaghaie, R., Saeri, M.R., Azizi, M., 2015. Synthesis, characterization and biocompatibility of silver nanoparticles synthesized from *Nigella sativa* leaf extract in comparison with chemical silver nanoparticles. Ecotoxicol. Environ. Saf. 120, 400-408. https://doi.org/10.1016/j.ecoenv.2015.06.025

Anu, K., Singaravelu, G., Murugan, K., Benelli, G., 2017. Green-synthesis of selenium nanoparticles using garlic cloves (*Allium sativum*): Biophysical characterization and cytotoxicity on Vero cells. J. Clust. Sci. 28, 551-563. https://doi.org/10.1007/s10876-016-1123-7

Applerot, G., Lipovsky, A., Dror, R., Perkas, N., Nitzan, Y., Lubart, R., Gedanken, A., 2009. Enhanced antibacterial activity of nanocrystalline ZnO due to increased ROS-mediated cell injury. Adv. Funct. Mater. 19(6), 842-852. https://doi.org/10.1002/adfm.200801081

Baka, Z.A.M., El-Sharkawy, A.M., El-Zahed, M.M., 2024. Anti-*Aspergillus niger* action of biosynthesized silicon dioxide nanoparticles alone or combined with *Matricaria chamomilla* L. extract. J. Microbiol. Biotechnol. Food Sci. 13(5), e10816. https://doi.org/10.55251/jmbfs.10816

Beheshti, N., Soflaei, S., Shakibaie, M., Yazdi, M.H., Ghaffarifar, F., Dalimi, A., Shahverdi, A.R., 2013. Efficacy of biogenic selenium nanoparticles against *Leishmania major*: *In vitro* and *in vivo* studies. J. Trace Elem. Med. Biol. 27(3), 203-207. https://doi.org/10.1016/j.jtemb.2012.11.002

Chen, X., Schluesener, H.J., 2008. Nanosilver: A nanoproduct in medical application. Toxicol. Lett. 176(1), 1-12. https://doi.org/10.1016/j.toxlet.2007.10.004

CLSI (Clinical and Laboratory Standards Institute), 2000. Methods for dilution antimicrobial susceptibility test for bacteria that grow aerobically. Wayne, Pennsylvania, USA. M45.

CLSI, 2017. Performance standards for antimicrobial susceptibility testing: Approved standard-twenty-seven Edition. Clinical and Laboratory Standards Institute, Wayne, Pennsylvania, USA. M100-S26.

Da Silveira, A.T., 2018. Bioactive compounds and health benefits of some palm species traditionally used in Africa and the Americas–a review. J. Ethnopharmacol. 224, 202-229. https://doi.org/10.1016/j.jep.2018.05.035

De Lagarde, M., Vanier, G., Arsenault, J., Fairbrother, J.M., 2021. High risk clone: A proposal of criteria adapted to the one health context with application to enterotoxigenic *Escherichia coli* in the pig population. Antibiotics 10(3), 244. https://doi.org/10.3390/antibiotics10030244

Dewir, Y.H., El-Mahrouk, M.E., Seliem, M.K., Murthy, H.N., 2021. Bioactive compounds of California fan palm *Washingtonia filifera* (Linden ex André) H. Wendl. ex de Bary. In: Murthy, H., Bapat, V. (Eds.) Bioactive compounds in underutilized fruits and nuts. Reference series in phytochemistry. Springer, Cham. https://doi.org/10.1007/978-3-030-30182-8_7

Elbestawy, M.K., El-Sherbiny, G.M., Moghannem, S.A., Farghal, E.E., 2023. Antibacterial, antibiofilm, and anti-inflammatory activities of ginger extract against *Helicobacter pylori*. J. Microbiol. Res. 14(3), 1124-1138. https://doi.org/10.3390/microbiolres14030075

El-Dein, M.M., Baka, Z.A., Abou-Dobara, M.I., El-Sayed, A.K., El-Zahed, M.M., 2021. Extracellular biosynthesis, optimization, characterization and antimicrobial potential of *Escherichia coli* D8 silver nanoparticles. J. Microbiol. Biotechnol. Food Sci. 10(4), 648-656. https://doi.org/10.15414/jmbfs.2021.10.4.648-656

El-Fallal, A.A., Elfayoumy, R.A., El-Zahed, M.M., 2023. Antibacterial activity of biosynthesized zinc oxide nanoparticles using Kombucha extract. SN Appl. Sci. 5(12), 332. https://doi.org/10.1007/s42452-023-05546-x

El-Zahed, M.M., Diab, M.A., El-Sonbati, A.Z., Nozha, S.G., Issa, H.R., El-Mogazy, M.A., Morgan, S.M., 2024. Antibacterial, antifungal, DNA interactions, and antioxidant evaluation of Cu (II) Co (II), Ni (II), Mn (II) and UO_2 (II) mixed ligand metal complexes: Synthesis, characterization and molecular docking studies. Mater. Sci. Eng.: B. 299, 116998. https://doi.org/10.1016/j.mseb.2023.116998

Fayed, R., Elnemr, A.M., El-Zahed, M.M., 2023. Synthesis, characterization, antimicrobial and electrochemical studies of biosynthesized zinc oxide nanoparticles using the probiotic *Bacillus coagulans* (ATCC 7050). J. Microbiol. Biotechnol. Food Sci. 13(3), e9962. https://doi.org/10.55251/jmbfs.9962

Foo, L.W., Salleh, E., Mamat, S.N., 2015. Extraction and qualitative analysis of *Piper betle* leaves for antimicrobial activities. Int. J. Eng. Sci. 2(2), 1-8. https://api.semanticscholar.org/CorpusID:51962042

Fouda, A., Al-Otaibi, W.A., Saber, T., AlMotwaa, S.M., Alshallash, K.S., Elhady, M., Badr, N.F., Abdel-Rahman, M.A., 2022. Antimicrobial, antiviral, and *in vitro* cytotoxicity and mosquitocidal activities of *Portulaca oleracea*-based green synthesis of selenium nanoparticles. J. Funct. Biomater. 13(3), 157. https://doi.org/10.3390/jfb13030157

Glover, R.L.K., Nyanganyura, D., Mufamadi, M.S., Mulaudzi, R.B., 2021. Green synthesis of nanoparticles from natural plant parts. In: Glover, R.L., Nyanganyura, D., Mufamadi, M.S., Mulaudzi, R.B. (Eds.) Green Synthesis in Nanomedicine and Human Health (1st ed.). pp.

342. CRC Press, Boca Raton. https://doi.org/10.1201/9781003023197

Gomaa, R.A., 2019. Physico-chemical characteristics of *Washingtonia robusta* fruit oil. SCUJ 6(1), 19-25.https://doi.org/10.21608/scuj.2019.60150

Hadrup, N., Lam, H.R., 2014. Oral toxicity of silver ions, silver nanoparticles and colloidal silver–a review Regul. Toxicol. Pharmacol. 68(1), 1-7. https://doi.org/10.1016/j.yrtph.2013.11.002

Huang, X., Chen, X., Chen, Q., Yu, Q., Sun, D., Liu, J., 2016. Investigation of functional selenium nanoparticles as potent antimicrobial agents against superbugs. Acta Biomater. 30, 397-407. https://doi.org/10.1016/j.actbio.2015.10.041

Khan, FA. (Ed.), 2020. Synthesis of nanomaterials: methods & technology. In: Applications of nanomaterials in human health (1st ed.). pp. 15–21. Springer, Singapore. https://doi.org/10.1007/978-981-15-4802-4_2

Lai, Y., Meng, M., Yu, Y., Wang, X., Ding, T., 2011. Photoluminescence and photocatalysis of the flower-like nano-ZnO photocatalysts prepared by a facile hydrothermal method with or without ultrasonic assistance. Appl. Catal. B: Environ 105(3-4), 335-345. https://doi.org/10.1016/j.apcatb.2011.04.028

Lee, M.K., Kim, T.G., Kim, W., Sung, Y.M., 2008. Surface plasmon resonance (SPR) electron and energy transfer in noble metal− zinc oxide composite nanocrystals. J. Phys. Chem. C 112(27), 10079-10082. https://doi.org/10.1021/jp8018809

Leisegang, K. (Ed.)., 2021. Herbal pharmacognosy: An introduction. In: Herbal medicine in andrology. pp. 17-26. Academic Press, Cambridge. https://doi.org/10.1016/B978-0-12-815565-3.00003-5

Mohamed, E.A., El-Zahed, M.M., 2024. Anticandidal applications of selenium nanoparticles biosynthesized with *Limosilactobacillus fermentum* (OR553490). Discover Nano 19(1), 115. https://doi.org/10.1186/s11671-024-04055-z

Mohammed, E.J., Abdelaziz, A.E., Mekky, A.E., Mahmoud, N.N., Sharaf, M., Al-Habibi, M.M., Khairy, N.M., Al-Askar, A.A., Youssef, F.S., Gaber, M.A., Saied, E., 2024. Biomedical promise of *Aspergillus flavus*-biosynthesized selenium nanoparticles: A green synthesis approach to antiviral, anticancer, anti-biofilm, and antibacterial applications. Pharmaceuticals 17(7), 915. https://doi.org/10.3390/ph17070915

Monte, J., Abreu, A.C., Borges, A., Simões, L.C., Simões, M., 2014. Antimicrobial activity of selected phytochemicals against *Escherichia coli* and *Staphylococcus aureus* and their biofilms. Pathogens 3(2), 473-498. https://doi.org/10.3390/pathogens3020473

Mosmann, T., 1983. Rapid colorimetric assay for cellular growth and survival: application to proliferation and cytotoxicity assays. J. Immunol. Methods. 65(1-2), 55-63. https://doi.org/10.1016/0022-1759(83)90303-4

Novak, A.F., Clark, G.C., Dupuy, H.P., 1961. Antimicrobial activity of some ricinoleic acid oleic acid derivatives. J. Am. Oil Chem. Soc. 38(6), 321-324. https://doi.org/10.1007/BF02638439

Prestinaci, F., Pezzotti, P., Pantosti, A., 2015. Antimicrobial resistance: A global multifaceted phenomenon. PGH 109(7), 309-318. https://doi.org/10.1179/2047773215Y.0000000030

Pu, Z.H., Zhang, Y.Q., Yin, Z.Q., Jiao, X.U., Jia, R.Y., Yang, L.U., Fan, Y.A., 2010. Antibacterial activity of 9-octadecanoic acid-hexadecanoic acid-tetrahydrofuran-3,4-diyl ester from neem oil. J. Agric. Sci. 9(8), 1236-40.https://doi.org/10.1016/S1671-2927(09)60212-1

Raina, S., Roy, A., Bharadvaja, N., 2020. Degradation of dyes using biologically synthesized silver and copper nanoparticles. Environ. Nanotechnol. Monit. Manag. 13, 100278. https://doi.org/10.1016/j.enmm.2019.100278

Saeed, H.M., Ferdosi, M.F., Khan, I.H., Javaid, A., Sultan, M.W., 2023. Antibacterial activity and GC–MS analysis of white flowers extract of Nerium oleander L. Int. J. Biol. Biotech. 20(1), 163-168. https://www.cabidigitallibrary.org/doi/full/10.5555/20230121039

Saleem, I., Rana, N.F., Tanweer, T., Arif, W., Shafique, I., Alotaibi, A.S., Almukhlifi, H.A., Alshareef, S.A., Menaa, F., 2022. Effectiveness of Se/ZnO NPs in enhancing the antibacterial activity of resin-based dental composites. Materials 15(21), 7827. https://doi.org/10.3390/ma15217827

Sánchez-López, E., Gomes, D., Esteruelas, G., Bonilla, L., Lopez-Machado, A.L., Galindo, R., Cano, A., Espina, M., Ettcheto, M., Camins, A., Silva, A.M., 2020. Metal-based nanoparticles as antimicrobial agents: An overview. Nanomaterials 10(2), 292. https://doi.org/10.3390/nano10020292

Selim, N.M., El-Hawary, S.S., El Zalabani, S.M., Shamma, R.N., Mahdy, N.E., Sherif, N.H., Fahmy, H.A., Mekkawy, M.H., Yasri, A., Sobeh, M., 2020. Impact of *Washingtonia robusta* leaves on gamma irradiation-induced hepatotoxicity in rats and correlation with STING pathway and phenolic composition. Pharmaceuticals 13(10), 320.

https://doi.org/10.3390/ph13100320

Sengul, A.B., Asmatulu, E., 2020. Toxicity of metal and metal oxide nanoparticles: A review. Environ. Chem. Lett. 18(5), 1659-1683. https://doi.org/10.1007/s10311-020-01033-6

Silva, A., Silva, V., Dapkevicius, M.D., Azevedo, M., Cordeiro, R., Pereira, J.E., Valentão, P., Falco, V., Igrejas, G., Caniça, M., Poeta, P., 2024. Unveiling antibiotic resistance, clonal diversity, and biofilm formation in *E. coli* isolated from healthy swine in Portugal. Pathogens 13(4), 305. https://doi.org/10.3390/pathogens13040305

Song, Y., Yang, F., Ma, M., Kang, Y., Hui, A., Quan, Z., Wang, A., 2022. Green synthesized Se–ZnO/attapulgite nanocomposites using *Aloe vera* leaf extract: Characterization, antibacterial and antioxidant activities. LWT 165, 113762. https://doi.org/10.1016/j.lwt.2022.113762

Tamanna, I.S., Gayathri, R., Sankaran, K., Veeraraghavan, V.P., Francis, A.P., 2024. Eco-friendly synthesis of selenium nanoparticles using *Orthosiphon stamineus* leaf extract and its biocompatibility studies. Bionanoscience 14(1), 37-44. https://doi.org/10.1007/s12668-023-01277-w

Tang, K.W., Millar, B.C., Moore, J.E., 2023. Antimicrobial resistance (AMR). Br. J. Biomed. Sci. 80, 11387. https://doi.org/10.3389/bjbs.2023.11387

Tiwari, P.M., Vig, K., Dennis, V.A., Singh, S.R., 2011. Functionalized gold nanoparticles and their biomedical applications. Nanomaterials 1(1), 31-63. https://doi.org/10.3390/nano1010031

Tiwari, S.K., Van der Putten, B.C., Fuchs, T.M., Vinh, T.N., Bootsma, M., Oldenkamp, R., La Ragione, R., Matamoros, S., Hoa, N.T., Berens, C., Leng, J., 2023. Genome-wide association reveals host-specific genomic traits in *Escherichia coli*. BMC Biol. 21(1), 76. https://doi.org/10.1186/s12915-023-01562-w

Tripathi, A.D., Mishra, R., Maurya, K.K., Singh, R.B., Wilson, D.W. (Eds.)., 2019. Estimates for world population and global food availability for global health. In: The role of functional food security in global health. pp. 3-24. Academic Press, Cambridge. https://doi.org/10.1016/B978-0-12-813148-0.00001-3

Tulinski, M., and Jurczyk, M., 2017. Nanomaterials synthesis methods. In: Mansfield, E., Kaiser, D.L., Fujita, D., Van de Voorde, M. (Eds.) Metrology and standardization of nanotechnology: protocols and industrial innovations. pp. 75–98. Wiley Online Library, New York. https://doi.org/10.1002/9783527800308.ch4

Venkatesh, R., Vidya, R., Kalaivani, K., 2014. Gas chromatography and mass spectrometry analysis of *Solanum villosum* (Mill) (Solanaceae). IJPSR 5(12), 5283-5287. https://www.cabidigitallibrary.org/doi/full/10.5555/20153042725

Wise, S.J.P., Goodale, B.C., Wise, S.S., Craig, G.A., Pongan, A.F., Walter, R.B., Thompson, W.D., Ng, A.K., Aboueissa, A.M., Mitani, H., Spalding, M.J., 2010. Silver nanospheres are cytotoxic and genotoxic to fish cells. Aquat. Toxicol. 97(1), 34-41. https://doi.org/10.1016/j.aquatox.2009.11.016

Xia, C., Liu, S., Cui, B., Li, M., Wang, H., Liang, C., Tran, P.A., Wang, Y., Zhou, H., Yang, L., 2022. *In situ* synthesis of zinc oxide/selenium composite for UV blocker application. Int. J. Appl. Ceram. Technol. 19(5), 2437-2449. https://doi.org/10.1111/ijac.14099

Xue, X.Y., Chen, Z.H., Xing, L.L., Ma, C.H., Chen, Y.J., Wang, T.H., 2010. Enhanced optical and sensing properties of one-step synthesized Pt–ZnO nanoflowers. J. Phys. Chem. C 114(43), 18607-18611. https://doi.org/10.1021/jp1070067

Zhang, T., Wang, L., Chen, Q., Chen, C., 2014. Cytotoxic potential of silver nanoparticles. Yonsei Med. J. 55(2), 283-291. https://doi.org/10.3349%2Fymj.2014.55.2.283.

الملخص العربي

عنوان البحث: النشاط الضد بكتيري لجسيمات أكسيد الزنك النانومترية الخضراء المصنعة باستخدام مستخلص ثمار واشنطونيا روبوستا

رولا محمد فايد[١]، زكريا عوض بقا[١]، محمد مرزوق الزاهد [١*]

[١]قسم النبات والميكروبيولوجي – كلية العلوم – جامعة دمياط – مصر.

تمثل العدوى البكتيرية مصدر قلق عالمي بالغ الأهمية وخاصة في القطاع الصحي، وغالبًا ما تؤدي إلى إطالة فترة العلاج الذاتي، وإطالة أوقات الشفاء، وأحيانا فشل العلاج، وارتفاع تكاليف الرعاية الصحية، إلى جانب زيادة معدلات الوفيات. ركزت جهود الأبحاث العلمية الأخيرة على تعزيز صحة الإنسان والاستدامة البيئية من خلال تقنيات التخليق المبتكرة. تقدم هذه الدراسة طريقة مباشرة وفعالة وقليلة التكلفة للتخليق الأخضر لجسيمات أكسيد الزنك النانومترية باستخدام مستخلص ثمار واشنطونيا روبوستا وبحثت في نشاطها المضاد للبكتيريا. خضع مستخلص ثمار واشنطونيا روبوستا للفصل الكيميائي باستخدام الكروماتوغرافيا السائلة عالية الأداء، مما أدى إلى عزل أربعة مستخلصات فرعية مميزة تم اختبارها للنشاط المضاد للبكتيريا ضد بكتيريا موجبة الجرام وسالبة الجرام. أظهر المستخلص الميثانولي أعلى النتائج المضادة للبكتيريا وتم تحليله للمركبات النشطة بيولوجيًا باستخدام كروماتوغرافيا الغازالمزود بمطياف الكتلة. كشف هذا التحليل عن وجود عشرة مكونات كيميائية حيوية، بما في ذلك الهكساسيلوكسان (٤٣,٢٨٪)، وحمض التيترا ديكونيك (١٢,٩٩٪)، وحمض الأوليك (١٠,١٢٪)، والهبتاسيلوكسان (٩,٨٣٪). تم استخدام هذا المستخلص الميثانولي في تخليق جسيمات أكسيد الزنك النانومترية. تم توصيف الجسيمات النانومترية الناتجة باستخدام تقنيات مختلفة، بما في ذلك التحليل الطيفي للأشعة فوق البنفسجية المرئية،والتحليل الطيفي للأشعة تحت الحمراء، وتحليل زيتا، والمجهر الإلكتروني النافذ (TEM). تم تقييم الفعالية المضادة للبكتيريا لجسيمات أكسيد الزنك النانومترية ضد ايشيريشيا كولاي، و باسيلس سيريس. تم تقييم النشاط المضاد للبكتيريا باستخدام طريقة انتشار المواد خلال الأجار، والحد الأدنى المثبط ، والتركيز المبيد للجراثيم. أشارت النتائج إلى أن جسيمات أكسيد الزنك النانومترية أظهرت نشاطًا مضادًا للبكتيريا جيدًا مع مناطق تثبيط متوسطة ١٨ ± ٠,٠٣ مم ضد ايشيريشيا كولاي، و٢٤ ± ٠,١٤ مم ضد باسيلس سيريس. كانت قيم الحد الأدنى للتركيز المثبط لجسيمات أكسيد الزنك النانومترية ٣٥ ميكروجرام/مل ضد ايشيريشيا كولاي و٢٥ ميكروجرام/مل ضد باسيلس سيريس. تطابقت قيم التركيز المبيد للجراثيم مع نتائج الحد الأدنى للتركيز المثبط والتي تتشير إلى التأثير القوي المبيد لجسيمات أكسيد الزنك النانومترية ضد الميكروبات.